remote sensing

MDPI

Article

Regulatory Impacts of the Three Gorges Dam on Long-Term Terrestrial Water Storage Anomalies in the Three Gorges Reservoir Area: Insights from GRACE and Multi-Source Data

Yu Zhang [1], Yi Zhang [2,*], Sulan Liu [1], Xiaohui Wu [1], Yubin Liu [2], Yulong Zhong [1] and Yunlong Wu [1,3,4]

[1] School of Geography and Information Engineering, China University of Geosciences, Wuhan 430074, China; 2575185080@cug.edu.cn (Y.Z.); sulanliu@cug.edu.cn (S.L.); wuxiaohui@cug.edu.cn (X.W.); zhongyl@cug.edu.cn (Y.Z.); wuyunlong@cug.edu.cn (Y.W.)
[2] Key Laboratory of Geological Survey and Evaluation of Ministry of Education, China University of Geosciences, Wuhan 430074, China; liuyb@cug.edu.cn
[3] Hubei Key Laboratory of Regional Ecology and Environmental Change, School of Geography and Information Engineering, China University of Geosciences, Wuhan 430079, China
[4] Hubei Luojia Laboratory, Wuhan 430079, China
* Correspondence: zhangyi11@cug.edu.cn

Abstract: Understanding the impact of human activities on regional water resources is essential for sustainable basin management. This study examines long-term terrestrial water storage anomalies (TWSA) in the Three Gorges Reservoir Area (TGRA) over two decades, from 2003 to 2023. The analysis utilizes data from the Gravity Recovery and Climate Experiment (GRACE) and its successor mission (GRACE-FO), complemented by Global Land Data Assimilation System (GLDAS) models and ECMWF Reanalysis v5 (ERA5) datasets. The research methodically explores the comparative contributions of natural factors and human activities to the region's hydrological dynamics. By integrating the GRACE Drought Severity Index (GRACE-DSI), this study uncovers the dynamics of droughts during extreme climate events. It also reveals the pivotal role of the Three Gorges Dam (TGD) in mitigating these events and managing regional water resources. Our findings indicate a notable upward trend in TWSA within the TGRA, with an annual increase of 0.93 cm/year. This trend is largely due to the effective regulatory operations of TGD. The dam effectively balances the seasonal distribution of water storage between summer and winter and substantially reduces the adverse effects of extreme droughts on regional water resources. Further, the GRACE-DSI analysis underscores the swift recovery of TWSA following the 2022 drought, highlighting TGD's critical role in responding to extreme climatic conditions. Through correlation analysis, it was found that compared with natural factors (correlation 0.62), human activities (correlation 0.91) exhibit a higher relative contribution to TWSA variability. The human-induced contributions were derived from the difference between GRACE and GLDAS datasets, capturing the combined effects of all human activities, including the operations of the TGD, agricultural irrigation, and urbanization. However, the TGD serves as a key regulatory facility that significantly influences regional water resource dynamics, particularly in mitigating extreme climatic events. This study provides a scientific basis for water resource management in the TGRA and similar large reservoir regions, emphasizing the necessity of integrating the interactions between human activities and natural factors in basin management strategies.

Keywords: GRACE/GRACE-FO; Three Gorges Dam; terrestrial water storage anomaly; human factors

check for updates

Academic Editor: Gabriel Senay

Received: 25 January 2025
Revised: 24 February 2025
Accepted: 1 March 2025
Published: 4 March 2025

Citation: Zhang, Y.; Zhang, Y.; Liu, S.; Wu, X.; Liu, Y.; Zhong, Y.; Wu, Y. Regulatory Impacts of the Three Gorges Dam on Long-Term Terrestrial Water Storage Anomalies in the Three Gorges Reservoir Area: Insights from GRACE and Multi-Source Data. *Remote Sens.* **2025**, *17*, 901. https://doi.org/10.3390/rs17050901

Copyright: © 2025 by the authors. Licensee MDPI, Basel, Switzerland. This article is an open access article distributed under the terms and conditions of the Creative Commons Attribution (CC BY) license (https://creativecommons.org/licenses/by/4.0/).

1. Introduction

The variability of global terrestrial water storage (TWS) serves as a critical indicator for assessing the impacts of human activities and climate change on water resources. As global climate change intensifies, extreme weather events such as droughts and floods have become increasingly frequent, exacerbating the uneven distribution of water resources worldwide [1,2]. Although recent studies have emphasized that natural lakes dominate global water storage changes due to their vast spatial extent and sensitivity to climate-driven hydrological cycles [3–5], human activities, including agricultural irrigation, industrial water use, and urbanization, have significantly intensified the imbalance between water supply and demand [6]. Continuous monitoring and precise investigation of global water cycle dynamics are crucial for modern water resource management and ecological conservation. However, traditional hydrological observation methods face limitations such as insufficient spatial coverage and restricted regional applicability, making it challenging to comprehensively capture water resource changes at both global and regional scales. To address these challenges, scientists have developed innovative methods based on gravity satellite technology [7]. The Gravity Recovery and Climate Experiment (GRACE) and its follow-on mission (GRACE-FO), jointly developed and managed by National Aeronautics and Space Administration (NASA) and the German Aerospace Center (DLR), have revolutionized the monitoring of TWS variations at global and regional scales [8]. Previous studies have shown that GRACE and GRACE-FO are highly effective in capturing TWS changes, especially in drought-prone regions and areas with intensive agricultural irrigation [9–14], providing essential data for precise water resource management [15]. Advancements in remote sensing technologies have further expanded the capabilities of hydrological monitoring. For example, photon-counting LiDAR has enhanced the ability to detect dynamic spatial changes with high precision [16], while methodologies such as weighted sparse models combined with shadow characteristics have improved detection accuracy in complex environments, as demonstrated in side-scan sonar applications [17]. These innovations highlight the growing potential of remote sensing tools in addressing diverse environmental challenges. Additionally, satellite altimetry has been instrumental in accurately measuring surface water height variations, particularly in flat terrain and oceanic regions, further supporting comprehensive hydrological assessments [18,19]. The widespread application of hydrological models and datasets has further advanced TWS research, significantly improving the spatial and temporal resolution of hydrological process studies. These advancements have provided new insights into the complex impacts of climate change and human activities on the water cycle, facilitating a deeper understanding of water resource dynamics in the context of global change [20].

Against the backdrop of intensified climate change, increasingly frequent extreme weather events, and escalating human activities, evaluating regional water resource dynamics and their driving mechanisms is critical for effective water resource management and ecological conservation. The Yangtze River Basin (YRB), one of the most vital water resource systems in China and globally, is profoundly influenced by both climate change and human activities [21–23]. Within the YRB, the Three Gorges Reservoir Area (TGRA) holds a unique geographical and hydrological significance. The region has a complex topography and a humid subtropical monsoon climate, with annual precipitation concentrated from May through September. This seasonal precipitation pattern leads to significant fluctuations in river flow and natural water storage. These natural hydrologic features have historically shaped the availability and distribution of water resources in the region. The construction and operation of the Three Gorges Dam (TGD), the world's largest water resources project, has resulted in more complex hydrologic processes and significant hydrodynamic variability in the region [24–26]. Although the water storage changes in natural lakes are primarily

driven by climatic factors, reservoirs are influenced by a combination of operational management, upstream water transfers, and extreme climate events [27,28]. This dual control by both natural variation and human intervention means that the operation of the TGD not only significantly influences the spatiotemporal distribution of regional water resources but also exerts far-reaching impacts on downstream ecosystems, socio-economic systems, and environmental conditions. In reservoir systems, human activities such as dam operation, irrigation withdrawals, and urbanization can either amplify or mitigate the natural variability of water storage. For instance, water storage in reservoirs is often increased artificially during dry periods to reduce the impact of droughts. However, extreme climate events like floods or droughts can strain operational capacity and alter long-term water storage trends. Therefore, a comprehensive investigation into the water resource variations and their driving factors in the TGRA is essential for scientifically managing and conserving water resources across the YRB.

Numerous studies have effectively utilized GRACE data to capture TWS variations in the YRB and assess the impacts of the TGD. For instance, GRACE-based research has played a critical role in monitoring water storage changes across major basins [13,29–32]. The introduction of the "Dam Impact Index" has provided a quantitative method to evaluate the influence of TGD operations on hydrological droughts in the YRB [33]. GRACE data have also been used to estimate groundwater changes before and after the construction of the TGD, revealing significant shifts in groundwater storage patterns [34]. Further studies indicate that human activities contribute to more than 50% of the observed groundwater changes [35]. Additionally, recent research employing GRACE data has highlighted the seasonal TWS variations in the YRB, emphasizing the role of reservoirs in regulating seasonal hydrological dynamics [36,37]. Collectively, these studies underscore the effectiveness of GRACE data in identifying the impacts of TGD on TWS changes within the YRB.

However, GRACE data are constrained by their spatial resolution (approximately 300 km), which limits their ability to provide detailed local hydrological information. To address this limitation, the ECMWF Reanalysis v5 (ERA5) and Global Land Data Assimilation System (GLDAS) datasets offer essential supplements for studying water resource dynamics at basin and regional scales through their high-resolution temporal series and extensive spatial coverage [33,38–40]. The ERA5 dataset, developed by the European Centre for Medium-Range Weather Forecasts (ECMWF), provides high spatial and temporal resolution, enabling the effective capture of extreme hydrological events and broader meteorological trends within the basin. For example, ERA5 data have been instrumental in providing meteorological context for studies on floods and droughts in the YRB [41]. The GLDAS model integrates diverse observational data and model simulations to generate high-resolution terrestrial hydrological data, which has been widely applied to track TWS variations and address the limitations of GRACE observations [42,43]. The comprehensive spatial coverage and temporal consistency of ERA5 and GLDAS make them important tools for evaluating TWS changes in the TGRA.

Although the impacts of human activities on water resources have been extensively studied [44,45], existing research primarily focuses on the direct consumption of water resources. In contrast, studies on the influence of large-scale hydraulic engineering projects, particularly their interactions with natural factors and their effects on the spatiotemporal distribution of water resources, remain relatively limited [46,47]. This study focuses on the TGRA and integrates GRACE, ERA5, and GLDAS datasets to comprehensively evaluate TWSA variations in the region, providing a scientific basis for dynamic water resource management within the basin.

In this study, we integrated GRACE and GRACE-FO data with ERA5, GLDAS, and in situ water level measurements to systematically analyze the long-term TWSA variations

in the TGRA over the period 2003–2023. TWSA estimates were derived using preprocessing operations such as Gaussian filtering and decorrelation processing to enhance data quality (see Sections 2.2 and 3.1 for details) [48–50]. Building on this foundation, the GRACE Drought Severity Index (GRACE-DSI) was employed to evaluate the impact of dam operations on mitigating droughts within the basin. Additionally, correlation analysis was performed to identify the statistical relationships between TWSA and natural and anthropogenic factors. This analysis quantified their respective contributions to basin-wide TWSA changes. The research workflow is depicted in Figure 1.

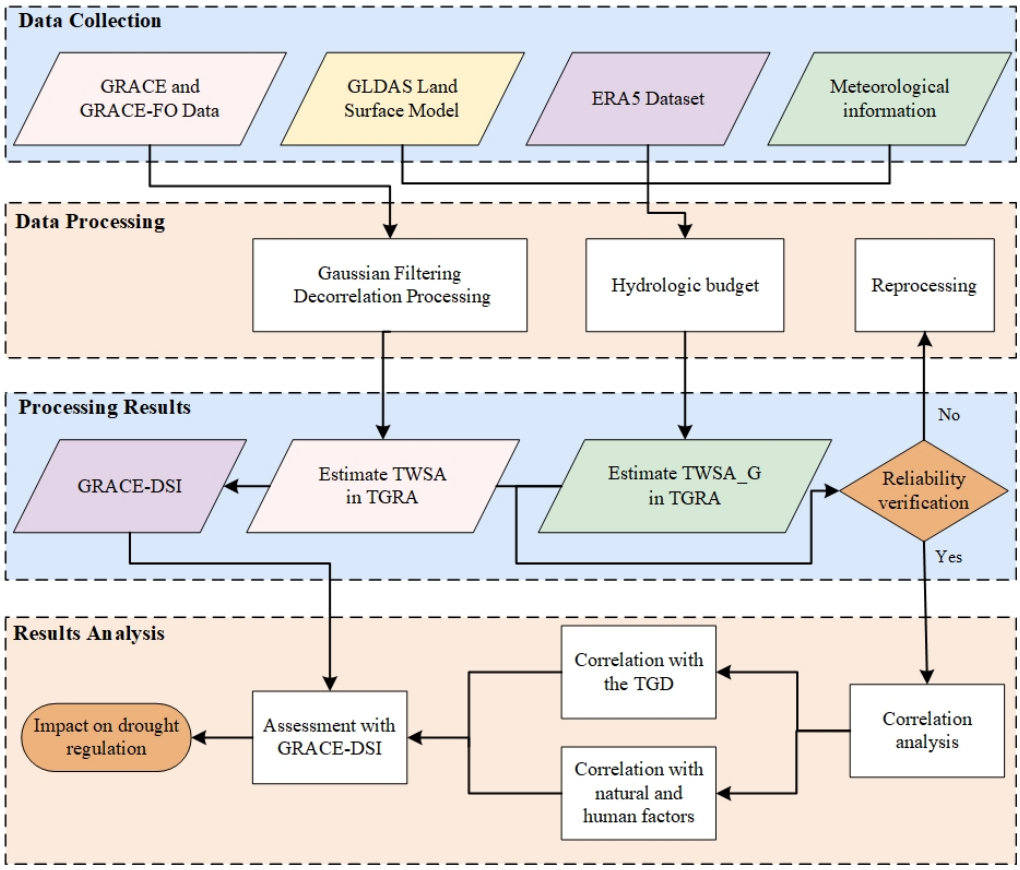

Figure 1. Analysis flow chart of water resources reserve change in the TGRA.

2. Materials

2.1. Study Area

The TGRA, located in the middle and upper reaches of the Yangtze River in China, spans latitudes 29°N to 32°N and longitudes 105°E to 112°E, covering a total area of approximately 60,000 km^2. The region is characterized by a subtropical humid monsoon climate, with the majority of annual precipitation occurring between May and September. It has the world's largest hydraulic engineering project—the TGD (Figure 2). The construction of the TGD officially started in December 1994 and passed the completion and acceptance in September 2015. Due to its complex terrain and unique geographical position, the construction and operation of the TGD have exerted significant influences on TWSA within the area [51].

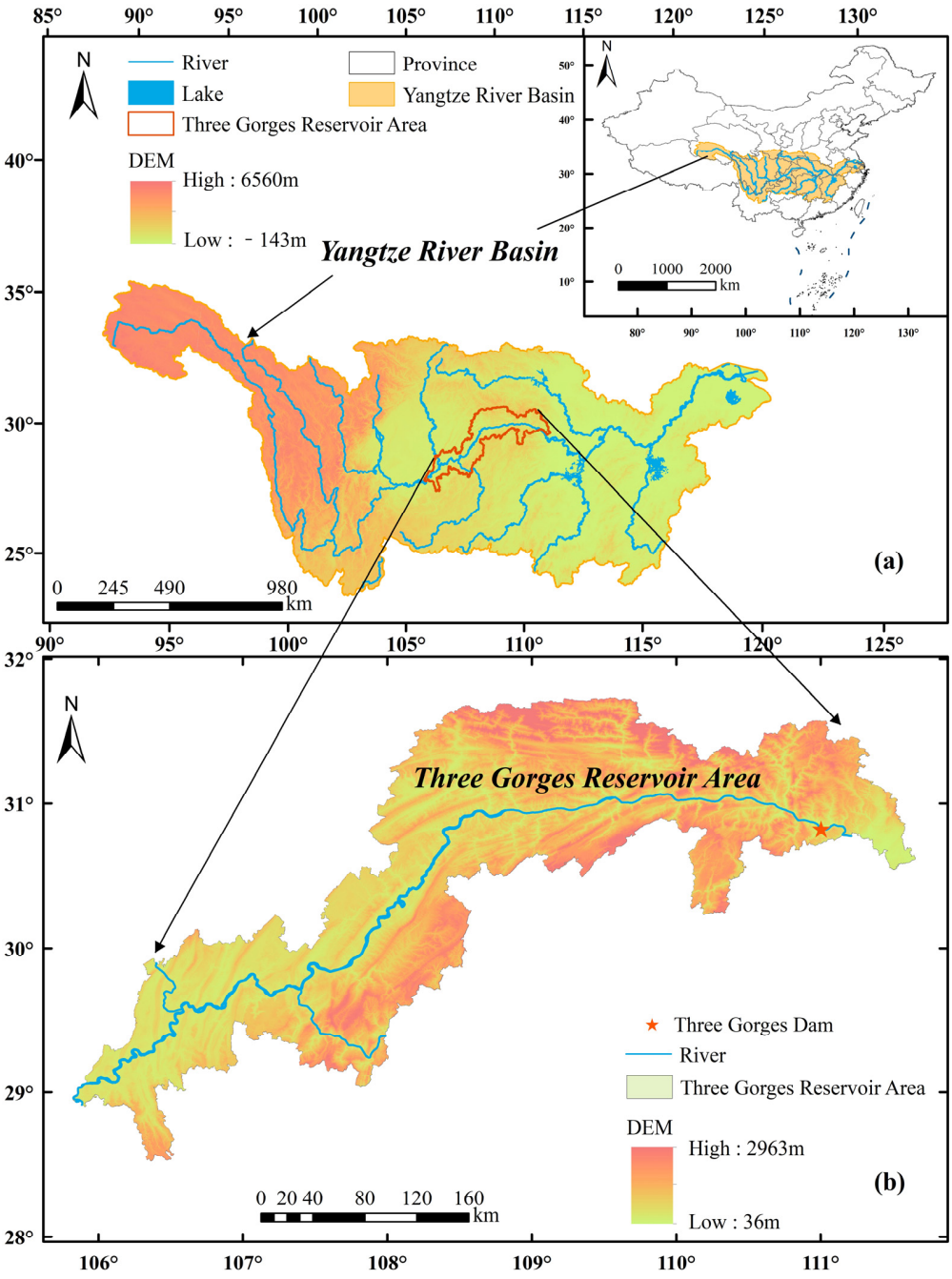

Figure 2. Location of the research area and related watersheds ((**a**) the location of the Yangtze River basin; (**b**) the location of the TGRA).

2.2. GRACE Data

This study utilizes GRACE and GRACE-FO satellite data, jointly provided by NASA and the DLR. The Level-2 Release 06 (RL06) data products processed by the Center for Space Research (CSR) at the University of Texas at Austin were employed. These datasets are freely accessible via the following URLs: ftp://isdcftp.gfz-potsdam.de/grace/Level-2/CSR/RL06/ and ftp://isdcftp.gfz-potsdam.de/grace-fo/Level-2/CSR/RL06/, accessed on 1 September 2024 [52,53].

The data span from January 2003 to December 2023, with a monthly temporal resolution. The spatial resolution is set at 0.25° × 0.25°. The spherical harmonic coefficients are truncated at degree and order 60, and data processing procedure steps are conducted to enhance data quality. These steps include the following:

(1) Replacing low-degree coefficients to correct for systematic errors.
(2) Filling data gaps during the GRACE mission period and addressing the discontinuity between GRACE and GRACE-FO missions using the Singular Spectrum Analysis (SSA) method [54].
(3) Reducing random errors and north-south striping noise in the raw spherical harmonic coefficients through decorrelation processing and the application of a 300 km Gaussian filter [48,49].
(4) To address signal leakage caused by filtering and truncation, a constrained forward modeling approach was applied to restore the true signal amplitude, thereby significantly improving data quality [55].

2.3. GLDAS and ERA5 Data

The GLDAS is designed to ingest satellite- and ground-based observational data products, leveraging advanced land surface modeling and data assimilation techniques to generate optimal fields of land surface states and fluxes. As a global terrestrial data assimilation system, GLDAS provides soil moisture, total canopy water storage, and snow water equivalent datasets for this study [56,57]. This study utilizes the GLDAS_NOAH025_M model, which offers monthly data with a spatial resolution of 0.25°, covering the period from 2003 to 2023. The dataset can be accessed through NASA's Goddard Earth Sciences Data and Information Services Center (GES DISC) at https://disc.gsfc.nasa.gov/datasets?keywords=GLDAS%20NOAH&page=1, accessed on 1 September 2024.

The ERA5 dataset, provided by the ECMWF, represents the fifth-generation global climate and weather reanalysis, covering the past 80 years. It offers monthly averaged data from 1940 to the present at a spatial resolution of 0.25°, replacing the previous ERA-Interim reanalysis dataset. ERA5 is widely used for capturing extreme hydrological events and meteorological trends. This study primarily relies on ERA5 data for snow depth and volumetric soil water layer information. The dataset is freely available at https://cds.climate.copernicus.eu/datasets/reanalysis-era5-single-levels-monthly-means?tab=overview, accessed on 1 September 2024.

2.4. 1 Km Monthly Precipitation Dataset for China

The 1 km monthly precipitation dataset for China provides high-resolution precipitation data from 2003 to 2023, with a spatial resolution of 0.008333° and precipitation measurements recorded in 0.1 mm increments [58]. This dataset was employed to analyze the correlation between precipitation and TWSA. The dataset is accessible at https://www.tpdc.ac.cn/en/data/faae7605-a0f2-4d18-b28f-5cee413766a2, accessed on 1 September 2024.

2.5. Observed Water Level Data of the TGD

Historical water level data for the TGD were obtained from the following website: http://xxfb.mwr.cn/hh_hs.html, accessed on 1 September 2024, covering the period from August 2003 to December 2023. These records include daily measurements of water levels, reservoir storage volumes, and discharge flows. Monthly water level data were derived by aggregating and averaging daily measurements and were used to analyze the relationship between TGD operations and TWSA variations.

3. Methodology

3.1. TWSA Inversion Based on GRACE Data

The estimation of TWSA using GRACE data is typically expressed as Equivalent Water Height (EWH). This method primarily utilizes the monthly Stokes coefficients recorded by the GRACE satellites, with the spherical harmonic coefficient technique being employed to sum and process the spherical harmonic functions. During this process, the long-term mean has been removed as the background field. By doing so, monthly variations in EWH—representing changes in terrestrial water storage—can be derived [52,59,60].

After decorrelation, filtering, and other preprocessing steps, GRACE data are used to derive the equation for inverting surface density changes:

$$\Delta\overline{\sigma}(\theta,\varphi) = \frac{2a\rho_{ave}\pi}{3}\sum_{l=0}^{\infty}\sum_{m=0}^{l}\overline{P}_{lm}(\cos\theta)\frac{2l+1}{1+k_l}W_l(\Delta C_{lm}\cos(m\varphi)+\Delta S_{lm}\sin(m\varphi)) \quad (1)$$

where a is the mean radius of Earth; φ and θ are the longitude and colatitude of the point of interest; and ρ_{ave} represents the mean density of the Earth, which is 5517 kg/m^3. ΔC_{lm} and ΔS_{lm} are the spherical harmonic coefficients corresponding to the observed values on the sphere after the background field has been removed; $\overline{P}_{lm}$ is the fully normalized associated Legendre function; l and m denote the degree and order; k_l is the elastic load Love number corresponding to degree l; and W_l represents the Gaussian smoothing function, which can effectively reduce high-frequency noise in GRACE data and eliminate part of the north–south stripes.

To minimize the influence of striping noise, this study applies a combined filter consisting of Gaussian smoothing with a radius of 300 km and a height decorrelation filter (P4M6). Additionally, constrained forward modeling methods are utilized to reconstruct the original signal strength, addressing signal attenuation caused by filtering and truncation.

The change in EWH is calculated from the change in surface density as follows [59]:

$$EWH(\theta,\varphi) = \frac{\Delta\overline{\sigma}(\theta,\varphi)}{\rho_w} \quad (2)$$

where ρ_w = 1000 kg/m^3.

Once the EWH is obtained, further analysis of its time series is necessary, including the identification of trends and seasonal variations (annual and semi-annual). To quantify the long-term trends and seasonal variations in the GRACE and GLDAS datasets, least-squares regression is employed to decompose the time series into a linear trend and annual and semi-annual cycles [61]. The decomposition is represented by the following equation:

$$EWH(\theta,\varphi,t) = \beta_0(\theta,\varphi)+\beta_1(\theta,\varphi)t+\beta_2(\cos(\omega_1 t+\alpha_1(\theta,\varphi))+\beta_3(\cos(\omega_2 t+\alpha_2(\theta,\varphi)) \quad (3)$$

where β_0, β_1, β_2, β_3, α_1, and α_2 are the parameters to be estimated in the least-squares regression model, with $\omega_1 = 2\pi$ representing the annual frequency and $\omega_2 = 4\pi$ representing the semi-annual frequency.

3.2. TWSA Estimates Based on GLDAS and ERA5 Data

TWSA can also be simulated using hydrological models and reanalysis datasets. This section focuses on two key sources: GLDAS and ERA5. Surface water storage derived from GLDAS is represented by changes in soil moisture, total canopy water storage, and snow water equivalent [15,62,63]. The equation is as follows:

$$TWSA_{GLDAS} = SMSA + CWSA + SWSA \quad (4)$$

In this formula, SMSA represents Soil Moisture Storage Anomaly, including changes in moisture across different depth layers (e.g., 0–10 cm, 10–40 cm, 40–100 cm, and 100–200 cm). CWSA denotes Canopy Water Storage Anomaly. SWSA refers to Snow Water Equivalent Anomaly. During this process, remove the long-term mean as the background field.

In addition to GLDAS, TWSA can be estimated using the ERA5 dataset. ERA5 TWS is computed as the sum of total column soil moisture (consisting of four layers: 0–7 cm, 7–28 cm, 28–100 cm, and 100–255 cm) and snow depth. However, due to limitations in the model structure, certain water storage components are excluded, resulting in a less comprehensive description compared with GLDAS.

Anomalies in the ERA5 TWS data are calculated by subtracting the long-term mean for each pixel over the period from January 2003 to December 2023. This approach facilitates direct comparisons with GRACE-observed TWSA data, enabling the assessment of hydrological trends over time.

3.3. Natural and Human Factors Affecting TWSA

To evaluate the impact of human activities on TWSA in the TGRA, it is crucial to distinguish between the contributions of natural and anthropogenic factors [64–66]. In this study, natural factors influencing TWSA were primarily linked to climatic variables such as precipitation and evapotranspiration, which were quantified using hydrological model outputs from the GLDAS and ERA5 datasets. These models provide estimates of water storage changes driven by natural processes.

The human-induced component of TWSA ($TWSA_h$) was calculated as the difference between the total anomaly in terrestrial water storage derived from GRACE ($TWSA$) observations and the anomaly attributed to natural factors ($TWSA_c$):

$$TWSA_h = TWSA - TWSA_c \tag{5}$$

Here, $TWSA$ represents the total terrestrial water storage anomaly obtained through GRACE satellite inversion. $TWSA_c$ refers to the portion of TWSA driven by natural processes, as simulated by hydrological models. This approach allowed us to isolate the influence of human activities, such as reservoir operations, on water storage changes in the study area.

3.4. Drought Index GRACE-DSI

The GRACE-DSI is based solely on satellite-derived gravity measurements, enabling consistent global monitoring of drought conditions, even in areas with limited ground-based observational data. This index is calculated by converting TWSA into GRACE-DSI, with the conversion equation expressed as follows [67]:

$$GRACE - DSI_{i,j} = \frac{TWSA_{i,j} - TWSA_j^{mean}}{\sigma_j} \tag{6}$$

where $TWSA_{i,j}$ represents the TWSA for a specific year i and month j within the period from 2003 to 2023. $TWSA_j^{mean}$ and σ_j denote the temporal mean and standard deviation of TWSA for month j, respectively.

4. Results

4.1. Characteristics of Spatial and Temporal Changes in TWSA in the TGRA

4.1.1. Long-Term Trends of TWSA

To investigate the temporal characteristics of TWSA in the TGRA from January 2003 to December 2023, we calculated and analyzed long-term TWSA time series. The results

are presented in Figure 3. During data processing, gaps in the GRACE and GRACE-FO missions were interpolated using the SSA method, effectively bridging the discontinuities between the two missions and ensuring the completeness and continuity of the time series. Figure 3 illustrates the TWSA trends derived from GRACE, GRACE-FM (corrected for leakage errors using forward modeling), and the GLDAS model. The GRACE-FM results show high consistency with GRACE data in terms of trends but exhibit a larger amplitude range of −21 cm to 24 cm. The Mann–Kendall (M-K) trend test, with a statistic of $Z = 4.92$ and a p-value < 0.001, passed the 99% confidence interval and confirmed the statistical significance of the observed trends, highlighting the improved ability of GRACE-FM to capture dynamic water storage changes in the TGRA after correcting for leakage errors.

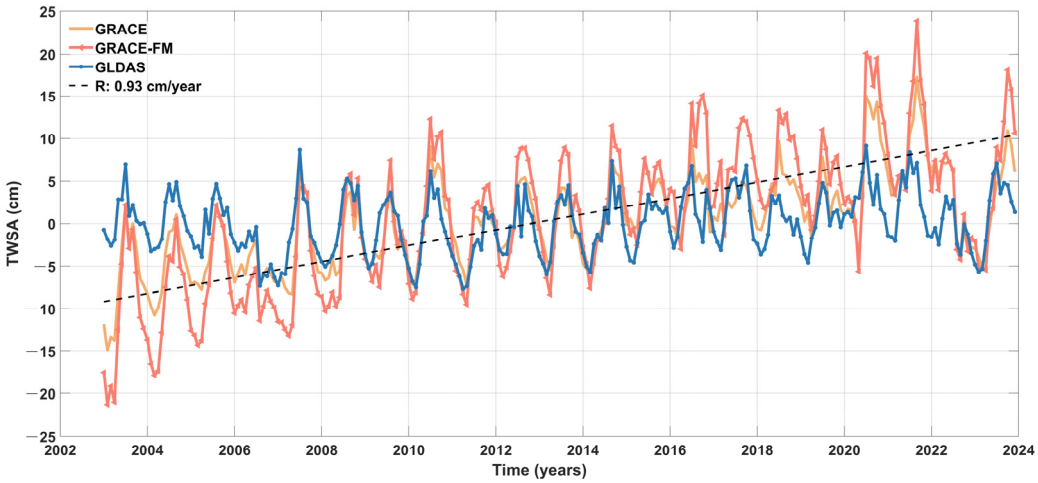

Figure 3. Comparison of TWSA derived from GRACE, GRACE-FM, and GLDAS datasets for the TGRA from 2003 to 2023. R represents the rate of change in TWSA reflected by GRACE-FM.

During the study period, GRACE-FM analysis revealed an average TWSA increase of 0.93 cm/year in the TGRA, reflecting the significant regulatory impact of the TGD on regional water resources. Meanwhile, TWSA trends derived from the GLDAS model also indicated an upward trend, with a more modest average increase of 0.14 cm/year. The discrepancy between GRACE and GLDAS data is likely attributable to the GLDAS model's primary focus on shallow surface water changes (e.g., soil moisture) while not accounting for contributions from groundwater and surface water bodies. Additionally, variability across different basins may contribute to the observed differences between the two datasets [68].

4.1.2. Seasonal Variations and Anomalies of TWSA

As precipitation is an important natural factor of TWSA fluctuations, it is important to examine how seasonal variations in precipitation correlate with TWSA trends [69]. The seasonal variations in precipitation exhibit a high degree of consistency with TWSA fluctuations derived from various datasets (Figure 4). Notably, precipitation changes exert a lagging effect on TWSA, typically delayed by 1–2 months. During summer (June–August), precipitation usually reaches its annual peak, significantly increasing TWSA due to the combined effects of delayed precipitation and evapotranspiration processes. Additionally, the reservoir's water storage capacity likely influences the amplitude of fluctuations during this period, as further quantified in Section 4.2 using reservoir operations data. In contrast, winter (December–February) experiences reduced precipitation, leading to a decline in TWSA.

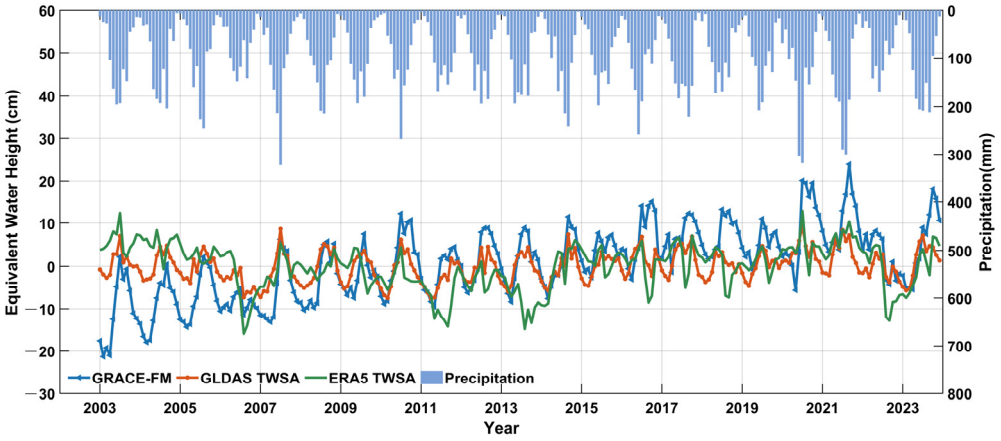

Figure 4. TWSA time series (2003–2023) for the TGRA derived from GRACE-FM, GLDAS, and ERA5, alongside precipitation data from 1 km monthly precipitation dataset for China.

Certain years with extreme climatic events had particularly pronounced impacts on TWSA. For example: In 2020, the region experienced the most severe flooding since 1998, with a sharp increase in summer precipitation causing frequent flooding events. In 2021, extreme rainfall led to unusual autumn floods in the upper Yangtze River during September–October. In 2022, insufficient summer precipitation caused a dramatic reduction in TGRA TWSA. While droughts affected other basins, the effective regulation by the TGD mitigated drought impacts within the TGRA.

Figure 5 further illustrates the seasonal variations in TWSA, categorized into spring (March–May), summer (June–August), autumn (September–November), and winter (December–February). The results reveal smaller fluctuations in TWSA during spring and winter, while summer and autumn exhibit more pronounced variability. The intense summer fluctuations are primarily driven by precipitation peaks, whereas the significant autumn fluctuations result from the combined effects of precipitation lag and TGD reservoir operations. These dynamic interactions demonstrate a strong coupling of natural precipitation patterns and human regulation, resulting in more complex seasonal TWSA variability.

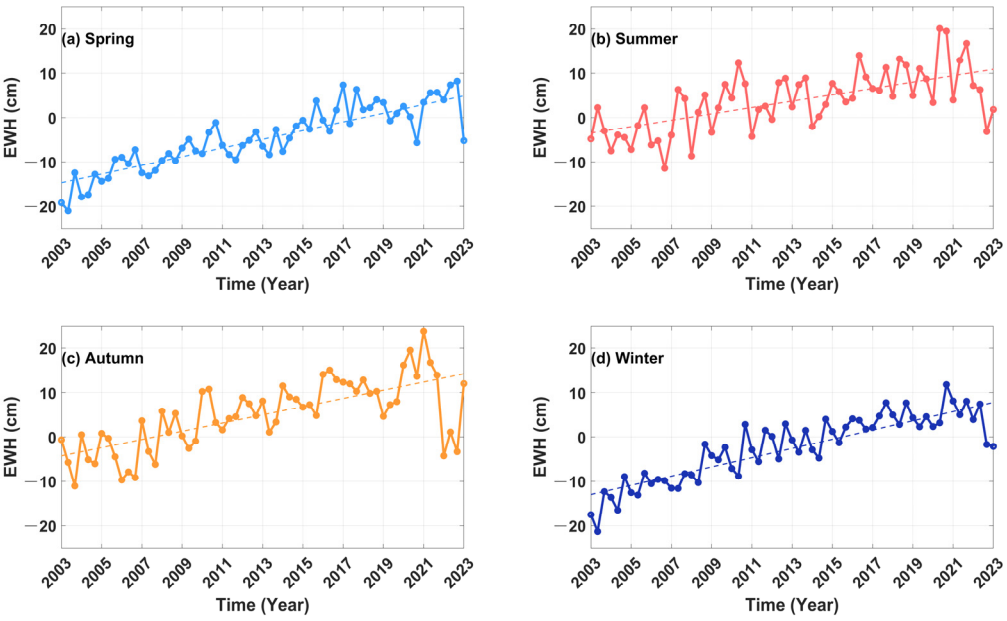

Figure 5. Seasonal variations in TWSA time series for the TGRA: (**a**) spring, (**b**) summer, (**c**) autumn, (**d**) winter.

Overall, the long-term trends indicate high consistency among GRACE-FM, GLDAS TWSA, and ERA5 TWSA results, with peaks and troughs aligning closely (Figure 4). However, the amplitudes of GLDAS and ERA5 are smaller than those of GRACE-FM. To further explore TWSA anomalies, we removed long-term trends and seasonal components from the time series (Figure 6). De-trending removes long-term variability driven by factors such as climate change and human activities, highlighting short-term deviations from expected trends. Deseasonalizing removes cyclical fluctuations caused primarily by the hydrological cycle (e.g., precipitation) and helps reveal non-seasonal anomalies and extreme hydrological events. The detrended and deseasonalized TWSA series reveals strong temporal consistency among GRACE-FM, GLDAS, and ERA5, though ERA5 exhibits larger amplitudes, particularly during negative anomalies in 2006, 2011, and 2013. Conversely, GRACE-FM captures more pronounced anomalies in 2022. These results suggest that ERA5 demonstrates higher sensitivity in detecting extreme hydrological events, while GRACE-FM provides a more comprehensive representation of overall water storage variations.

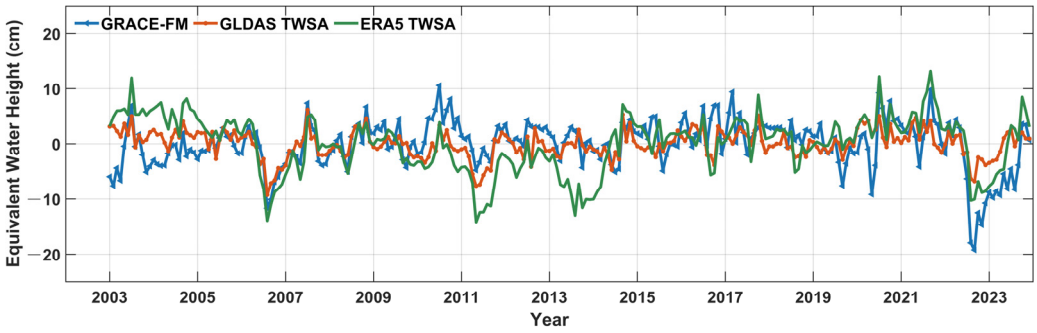

Figure 6. Detrended and deseasonalized TWSA series derived from GRACE-FM, GLDAS, and ERA5.

4.1.3. Spatial Distribution Characteristics and Regional Variations

To investigate the spatial distribution of TWSA under extreme climatic conditions, this study analyzed the TGRA region during the extreme rainfall event of September 2021 and the extreme drought event of September 2022, integrating data from GRACE, GRACE-FM, GLDAS, and ERA5 (Figure 7).

The GRACE data for September 2021 (Figure 7a) indicate that TWSA in the northeastern TGRA was significantly higher than in the southwestern region, suggesting greater terrestrial water storage in the northeast. This spatial pattern is further validated by GRACE-FM data (Figure 7c), which restored the signal and provided a clearer distribution, reinforcing the observation that TWSA in the northeast exceeds that in the southwest.

In contrast, the results for September 2022 (Figure 7b,d) reveal a significant reduction in overall TWSA across TGRA compared with September 2021, with the most pronounced decline in the northeastern region. However, GRACE-FM data (Figure 7d) demonstrate that, despite the overall reduction, the northeast maintained higher TWSA than the southwest. The characteristic of higher TWSA in the northeast region compared with the southwest region reflects that even under drought conditions, the areas near dams in the basin still have relatively higher wet signals than other regions. The GLDAS and ERA5 datasets (Figure 7e–h) show relatively weak variations in TWSA within the TGRA, while more pronounced anomalies are observed outside the basin, particularly in the northwest and southeast regions. The extreme drought event of 2022 led to a sharp reduction in TWSA, most notably in the northeastern region. This dramatic decline is much more evident in the GRACE and GRACE-FM data. However, even under extreme drought conditions, the TWSA within TGRA remains slightly higher than that in the areas outside the basin. Despite localized reductions in the northeastern TGRA (Figure 7f,h), the average TWSA in

TGRA is still relatively higher compared with the severe deficits observed in regions outside the basin. This highlights the ability of TGD to stabilize water storage in the reservoir area during extreme droughts.

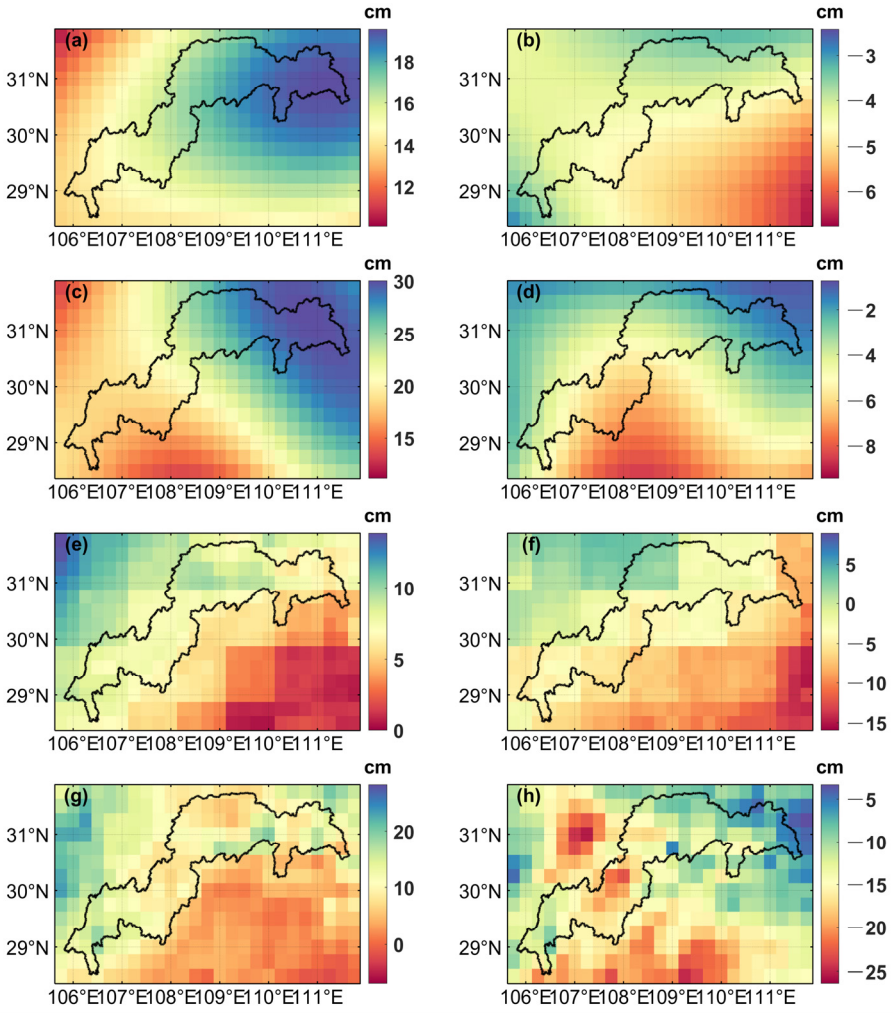

Figure 7. Spatial distribution of TWSA in TGRA based on different data sources. (**a**,**c**,**e**,**g**) represent the spatial distribution results of TWSA in the TGRA for September 2021, calculated using GRACE, GRACE-FM, GLDAS, and ERA5, respectively; (**b**,**d**,**f**,**h**) represent the spatial distribution results of TWSA in the TGRA for September 2022, calculated using GRACE, GRACE-FM, GLDAS, and ERA5, respectively.

4.2. Relative Contributions of Natural and Human Factors to TGRA TWSA

4.2.1. Interaction Between Natural Drivers and Reservoir Regulation

To quantitatively assess the impact of the TGD on TWSA variations in the TGRA region, historical water level data from TGD were compared with TWSA derived from GRACE, GRACE-FM, and GLDAS datasets (Figure 8). The analysis focuses on three key milestone events: first, the initial impoundment of the reservoir to 135 m in June 2003; second, the successful impoundment to 156 m in October 2006, which marked the commencement of the dam's operational phase; and finally, the extreme flood event in May–June 2020, which resulted in the highest recorded inflow since the reservoir's construction. The TGD project successfully passed completion and acceptance in September 2015, marking the full operational capacity of the dam and its associated infrastructure [70]. Temporal analysis shows slight delays (1–2 months) between the operational changes in the dam and corresponding TWSA responses. During the period from July 2003 to October 2006, GRACE-FM results indicate a modest upward trend in TGRA TWSA, with a rate of 0.22 cm/year,

corresponding to the reservoir's construction phase. From October 2006 to August 2020, TWSA exhibited a significantly higher growth rate of 1.00 cm/year, emphasizing the regulatory role of TGD in balancing regional water resources. The consistency between TGD water level adjustments and GRACE-derived TWSA trends (Figure 8) highlights the utility of reservoir operational data in validating the impact of satellite observations on regional hydrology. In contrast, the period from October 2020 to December 2023 saw a sharp decline in TWSA, at a rate of −2.95 cm/year, primarily driven by the extreme drought event in 2022. Minimum TWSA values of −4.25 cm and −3.70 cm were observed in GRACE-FM and GLDAS datasets, respectively.

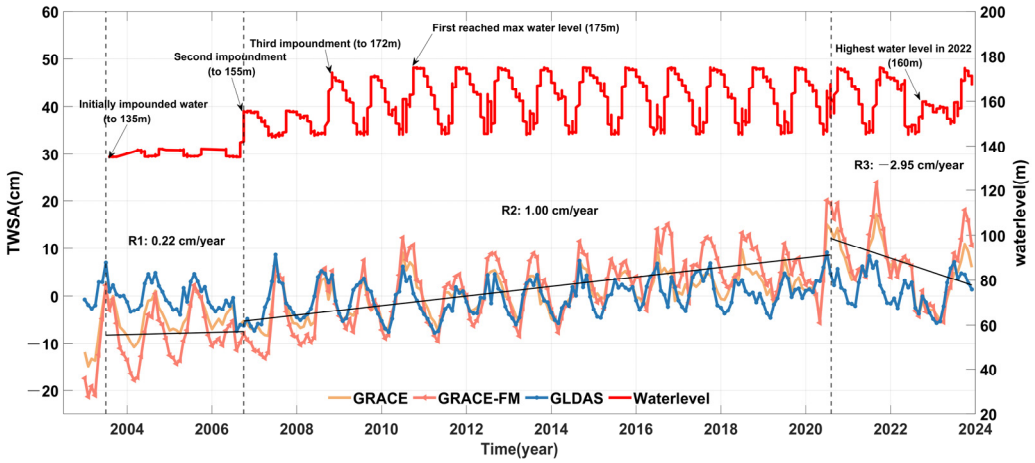

Figure 8. Changes in TGD water level and TWSA from GRACE, GRACE-FM, and GLDAS. The solid black line represents the trend of GRACE-FM for three periods: the first period from July 2003 to October 2006, the second from October 2006 to August 2020, and the third from August 2020 to December 2023. The dashed black lines indicate the time points separating the three periods: the first is July 2003, the second is October 2006, and the third is August 2020. Milestones for water storage are annotated.

As a seasonal regulating reservoir, TGD operates to release water prior to the flood season, reducing the water level to 145 m by June 10, and gradually refilling to its normal operational level of 175 m by late October. This operation is reflected in TWSA dynamics, where the annual summer peaks are influenced by both natural rainfall and dam regulation, while winter peaks are attributed to water storage from external basins.

From a seasonal perspective, TGD regulation interacts with natural precipitation in a complementary manner. During summer, peak precipitation coincides with dam operations to release water, yet GRACE TWSA still shows an increasing trend, likely due to the substantial contribution of precipitation exceeding the regulatory effect. Conversely, in winter, reduced precipitation is counteracted by reservoir storage, leading to smaller declines or even slight increases in TWSA. These findings demonstrate that TGD effectively buffers seasonal fluctuations in precipitation, stabilizing TWSA and mitigating natural disasters such as droughts and floods.

Figure 8 illustrates that the timing of peaks and troughs in GRACE, GRACE-FM, and GLDAS datasets is consistent, confirming their alignment in periodicity and phase, with GLDAS showing the smallest amplitude. Table 1 further supports this consistency through statistical metrics. From 2003 to 2023, TWSA in TGRA showed an overall upward trend, with an average annual increase of 0.92 cm. The annual amplitude dominated TWSA periodic variations, approximately four times larger than the semi-annual amplitude.

Table 1. Trends, seasonal variations, and cycle amplitudes from different data sources.

Dataset	Trend (cm/yr)	Annual Amplitude	Annual Phase (°)	Semi-Annual Amplitude	Semi-Annual Phase (°)
GRACE	0.57 ± 0.07	3.79 ± 0.57	237.91 ± 8.67	0.48 ± 0.57	35.33 ± 66.21
GRACE-FM	0.91 ± 0.09	6.02 ± 0.79	246.70 ± 7.51	0.66 ± 0.79	42.65 ± 42.88
GLDAS	0.12 ± 0.053	3.27 ± 0.45	217.65 ± 7.54	0.86 ± 0.45	312.37 ± 41.99

Segmented analysis of parameters also confirms these trends. From 2003 to August 2020, TWSA increased at rates of 0.61 cm/year (GRACE), 1.09 cm/year (GRACE-FM), and 0.12 cm/year (GLDAS). However, from August 2020 to December 2023, TWSA declined sharply at rates of −2.91 cm/year, −3.07 cm/year, and −0.74 cm/year, respectively. Precipitation showed a similar trend, rising by 0.80 cm/year during the first period and falling at −3.95 cm/year during the second, indicating that precipitation intensity was the primary driver of TWSA decline from 2020 to 2023.

4.2.2. Quantifying the Contributions of Natural and Human Factors to TGRA TWSA

The non-linear reservoir operations of the TGD significantly regulate TWSA in the TGRA, a process challenging to capture using traditional hydrological models such as GLDAS. However, GRACE satellite data effectively detect such regulatory effects. To quantify the relative contributions of natural factors and human activities to the hydrological processes in TGRA, we used the difference between TWSA derived from GRACE and GLDAS datasets as an approximation of human-induced contributions. It is important to note that this difference not only captures reservoir regulation signals but may also reflect groundwater dynamics and model errors, given the absence of groundwater processes and reservoir impacts in the GLDAS model.

Figure 9 presents the temporal series of TWSA driven by natural factors ($TWSA_c$) and human factors ($TWSA_h$), alongside their correlations with GRACE TWSA. $TWSA_c$ primarily captures water cycle processes dominated by precipitation and evapotranspiration, with peaks and troughs closely corresponding to seasonal precipitation dynamics. However, compared with GRACE data, $TWSA_c$ exhibits smaller amplitudes (Figure 9a), which can be attributed to the unaccounted contributions of processes beyond natural factors. This discrepancy highlights that GRACE data encompass not only natural contributions but also additional signals induced by human activities. Correlation analysis reveals a moderate relationship between $TWSA_c$ and GRACE TWSA (R = 0.62), indicating that natural factors alone do not fully explain the observed TWSA changes. This is likely due to GRACE capturing more complex hydrological processes, such as TGD regulation effects, groundwater changes, and atmospheric or hydrodynamic processes, underscoring the critical role of human activities in regulating hydrological dynamics.

Figure 9c,d further explore the relationship between GRACE TWSA and human-induced contributions ($TWSA_h$). As shown in Figure 9c, GRACE TWSA and $TWSA_h$ exhibit highly consistent trends and amplitudes, especially during reservoir filling and release periods. This synchronization underscores the substantial influence of long-term TGD regulation on regional water resource dynamics. Notably, during drought years such as 2022, reservoir operations significantly mitigated the adverse impacts of reduced precipitation on TWSA, as reflected in the pronounced positive deviation trend in $TWSA_h$.

This finding is reinforced by correlation analysis in Figure 9d, where GRACE TWSA and $TWSA_h$ achieve a high correlation coefficient (R = 0.91), demonstrating that human activities play a dominant role in driving TWSA changes over time in TGRA. However, it is worth noting that using the GRACE and GLDAS TWSA difference to approximate human-induced contributions introduces uncertainties. These include the limited sensitivity of

GLDAS to groundwater processes and reservoir dynamics and the spatial resolution constraints of GRACE. Future research should integrate high-resolution groundwater observation data and improved hydrological models to enhance the accuracy of human contribution quantification.

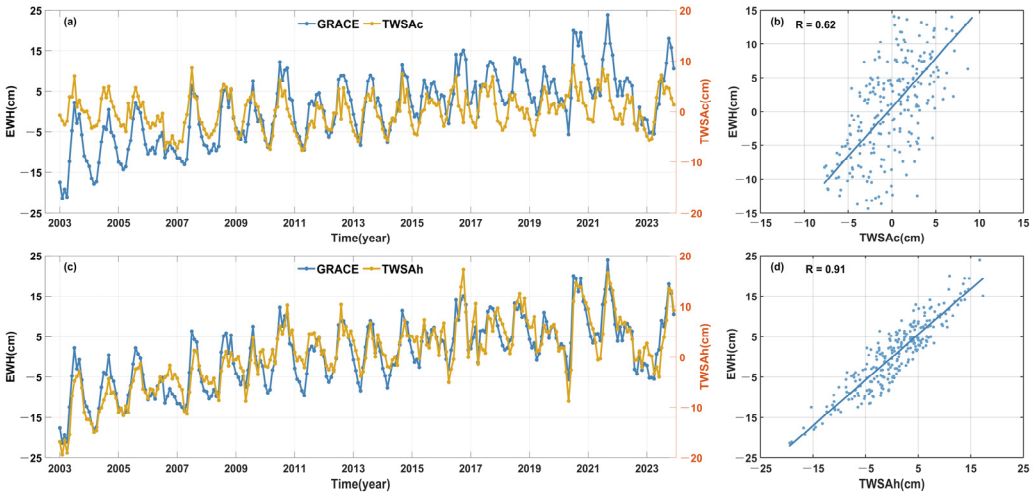

Figure 9. Time series and correlation analysis of GRACE data with natural and human TWSA. Note that the correlation coefficient R has no units ((**a**) GRACE data and time series of natural TWSA; (**b**) Correlation analysis between GRACE data and natural TWSA; (**c**) GRACE data and time series of artificial TWSA; (**d**) Correlation analysis between GRACE data and human TWSA).

To further investigate the critical role of TGD in hydrological regulation in the Yangtze River Basin, we analyzed the relationship between TGD reservoir storage changes and $TWSA_h$ (Figure 10). The reservoir volume was calculated using the following formula: $V = 0.2986 \times 1.0284^H$, where V (km^3) represents reservoir volume, and H (m) denotes the water level [71].

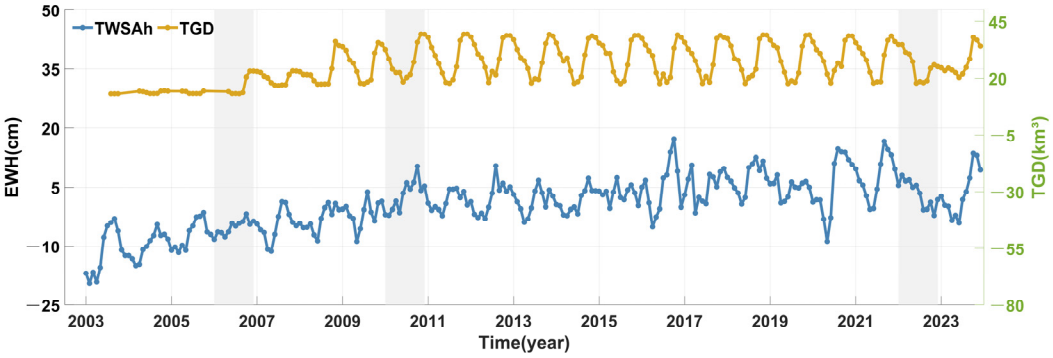

Figure 10. Time series relationship between TGD water storage and human-driven contributions. The shaded areas are 2006, 2010, and 2022, corresponding to TGD's trial operation phase, full operation phase, and an extreme drought event, respectively.

Key observations include the following:

In 2006, TGD was still in its trial operation phase, with limited regulatory capacity to mitigate the severe drought impacts of that year. This is reflected in the lower amplitude and lack of significant recovery trends in $TWSA_h$.

In 2010, TGD employed a dual strategy of flood release during the wet season and water storage during the dry season. This mechanism significantly improved the stability of regional water storage. Notably, during the autumn–winter storage period, cor-

responding $TWSA_h$ showed slight recovery trends, reflecting enhanced water resource management efficiency.

The extreme drought of 2022 further validated the critical role of TGD in hydrological regulation. While $TWSA_h$ exhibited a declining trend during the drought, reservoir operations effectively reduced the rate of decline. Furthermore, winter storage operations not only alleviated the drought's persistence but also contributed to a modest recovery in $TWSA_h$, showcasing the dam's capacity to regulate regional water storage under extreme climate conditions.

Overall, TGD's reservoir operations significantly enhanced autumn and winter water storage levels in the TGRA and played a vital role in mitigating the impacts of extreme climate events. These findings underscore the indispensable role of TGD in human-induced regulation within the basin.

5. Discussion

The GRACE-derived TWSA has demonstrated effectiveness in capturing large-scale water storage changes across China, including regions significantly impacted by human activities. Similar to the observations in this study, previous research has identified discrepancies between GRACE and model-based datasets such as GLDAS, which are likely due to differences in spatial resolution and model parameterization. GRACE data have also proven valuable in monitoring drought impacts and have shown high sensitivity to extreme hydrological anomalies. This study corroborates these findings by analyzing the unprecedented water storage deficits during the 2022 drought event in the TGRA, highlighting the critical role of GRACE in detecting and assessing hydrological extremes. Additionally, the regulatory role of the TGD in water storage management and downstream flood mitigation has been well established. The findings of this study not only align with earlier analyses but also extend them by examining the dam's regulatory effectiveness under extreme drought conditions, offering a deeper understanding of its long-term hydrological impacts.

To better evaluate the role of the TGD under extreme climatic conditions, this study calculated drought dynamics in the TGRA from 2003 to 2023 using the GRACE-DSI index (Figure 11). The GRACE-DSI, categorized into six levels ranging from "Exceptional Drought" to "Near Normal", offers a visual representation of drought dynamics through a color gradient. Table 2 details the corresponding thresholds for each drought level.

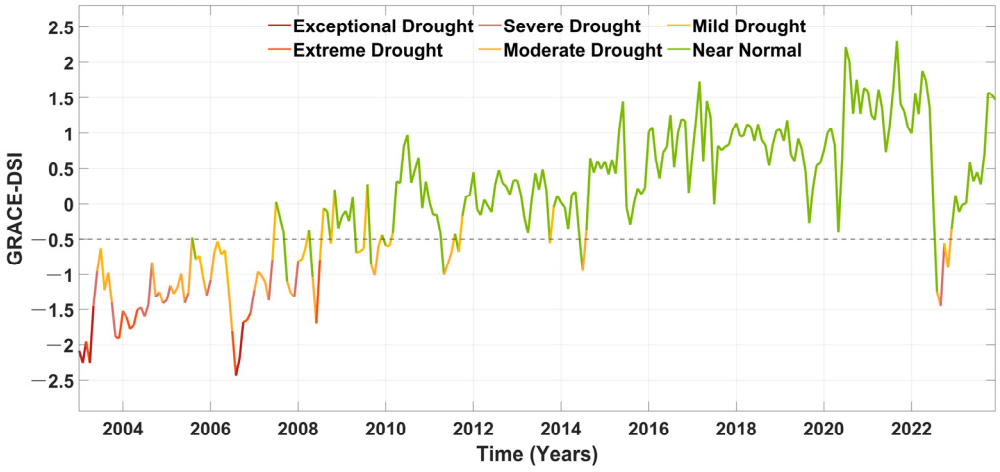

Figure 11. GRACE-DSI time series changes from January 2003 to December 2023 in TGRA. The gray dashed line indicates the critical value of the "Near-Normal" state. Note that the drought index corresponds to its starting point and the indices are dimensionless.

Table 2. GRACE-DSI classification.

Grades	GRACE-DSI	Grades	GRACE-DSI
Exceptional Drought	−2.00 or less	Moderate Drought	−1.29~−0.80
Extreme Drought	−1.99~−1.60	Mild Drought	−0.79~−0.50
Severe Drought	−1.59~−1.30	Near Normal	−0.49 or more

The segmentation clearly illustrates the temporal trends of drought severity, with red and orange regions concentrated primarily before 2010, reflecting more severe drought events during this period. Notably, the extreme drought in 2006 stands out, with GRACE-DSI values reaching their lowest levels. This period coincided with the construction and trial operation phase of the TGD, during which its regulatory capacity was not yet fully realized, resulting in limited spatial and temporal water resource allocation.

In contrast to 2006, the amplitude of the GRACE-DSI during the 2022 drought was relatively lower, indicating the enhanced regulatory capacity of the TGD. This improvement highlights the dam's progressive impact over time, with its operations providing significant mitigation of drought impacts in 2022. Furthermore, the rapid recovery of water resources in the aftermath of the 2022 drought further underscores the critical role of the TGD in maintaining hydrological stability under extreme conditions.

Since 2010, the prevalence of "Near-Normal" (green) and "Mild Drought" (yellow) conditions in the GRACE-DSI timeline demonstrates a significant alleviation of drought severity in the TGRA. This shift is closely linked to the continuous optimization of the TGD's regulatory operations. The precise adjustments during the autumn–winter storage and spring-summer release periods have substantially improved the dynamic management of regional water resources, enhancing the basin's resilience to natural climate variability.

Despite the occurrence of another extreme drought event in 2022, the GRACE-DSI results indicate that its impact was effectively controlled. By regulating the storage and distribution of water resources, the TGD significantly reduced the negative ecological and socio-economic impacts of the drought. The long-term trend observed in Figure 11 illustrates a clear reduction in both the frequency and intensity of extreme drought events within the basin following the TGD's operation, validating the sensitivity and applicability of GRACE-DSI in assessing drought dynamics and dam-regulation effects.

To further investigate the spatial characteristics of GRACE-DSI, we analyzed the spatial distribution of drought indices for critical months (May, August, and November) in 2006, 2010, and 2022 (Figure 12). The uniform color gradient reflects varying drought levels, with red representing severe drought and blue indicating water abundance. The horizontal arrangement of years and the vertical alignment of months provide a comparative perspective.

During the extreme drought in 2006, the TGD's trial operation phase resulted in limited regulatory effectiveness, failing to significantly alleviate drought impacts. In May, TGRA southern and central areas exhibited substantial water storage declines, indicating severe drought conditions. By August, the drought expanded both in intensity and coverage, encompassing the entire basin. This trend continued through November, highlighting severe water shortages during this period.

In 2010, due to the absence of extreme drought weather events during that period and the fact that TGD had entered the normal operation phase. Water storage in May gradually recovered to near-neutral levels, with August showing further improvements driven by the rainy season. By November, water distribution was more uniform, reflecting the dam's growing influence in mitigating hydrological variability.

The drought dynamics in 2022 were more complex, with much of the region already experiencing wet conditions by May. However, by August, extreme drought impacts became evident, particularly in localized areas with reduced water storage. Nonetheless, the rapid recovery observed in November underscores the TGD's effectiveness in balancing seasonal water distribution and mitigating the prolonged impacts of drought.

Comparisons across years for the same months of the same months across years reveal that drought severity from May to November 2006 was significantly higher than in 2010 and 2022. Additionally, the recovery speed in November 2022 far exceeded that of 2006, demonstrating the TGD's enhanced regulatory capabilities over time. Comparisons within the same year within the same year highlight the dam's pivotal role in increasing water storage during the rainy season and alleviating drought during non-rainy seasons.

The spatial distribution of water storage further reveals the sensitivity of the southern region of TGRA to extreme drought. The gradual recovery of water storage in the southern region between 2010 and 2022 reflects the combined influence of improved climate conditions and the TGD's optimized water management capacity.

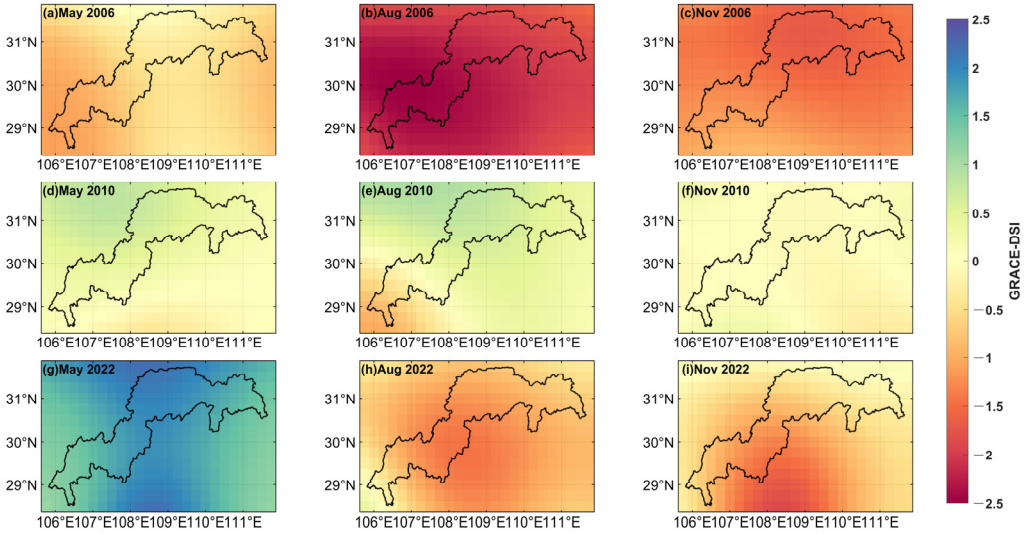

Figure 12. Spatial distribution of drought index in May, August, and November of TGRA in 2006, 2010, and 2022. Note that the indices are dimensionless.

6. Conclusions

This study systematically analyzed the TWSA dynamics in the TGRA from 2003 to 2023, utilizing data from GRACE, GRACE-FM, GLDAS, and ERA5. The research focused on quantifying the relative contributions of natural and anthropogenic factors to TWSA changes and employed the GRACE-DSI index to identify the spatiotemporal characteristics of extreme drought events. It also evaluated the critical role of the TGD in mitigating drought impacts and regulating regional hydrological dynamics. The results demonstrate a significant overall increase in TWSA, with GRACE-FM data indicating an annual rise of 0.93 cm/year, reflecting the significant regulatory effect of TGD on regional water resource dynamics since its operation. Seasonal TWSA fluctuations were closely linked to natural drivers such as precipitation and evapotranspiration, while TGD's reservoir operations significantly influenced summer and winter water storage distributions, ensuring seasonal water balance.

Under extreme climatic events, this study revealed notable variations in TGRA's TWSA and highlighted TGD's critical role in mitigating drought impacts. During the extreme drought of 2006, TGD's regulatory capacity was limited due to its trial operation phase, failing to effectively alleviate water shortages. In contrast, during the 2022 drought, the

operations of TGD significantly reduced the adverse impacts of drought on regional water resources, demonstrating its mature and efficient regulatory capabilities. GRACE-DSI analysis further revealed that TWSA recovery in November 2022 was markedly faster than in 2006, providing strong evidence of TGD's enhanced role in improving regional hydrological stability.

This study also quantitatively demonstrated the prominent contribution of anthropogenic factors, particularly TGD's regulatory role, to TWSA changes in TGRA. Compared with $TWSA_c$, driven by natural factors, $TWSA_h$ exhibited larger amplitudes and higher correlations, indicating that human-induced regulatory signals play a dominant role in the hydrological cycle. TGD's long-term operations not only proved advantageous in mitigating extreme climatic events but also played a pivotal role in balancing seasonal and non-seasonal water storage distributions. Such regulatory effects are critical for adapting to future extreme climatic conditions and ensuring water resource security in the basin.

In summary, this study comprehensively reveals the spatiotemporal characteristics and driving mechanisms of TWSA in the TGRA by integrating multi-source data and analytical methods, providing a scientific basis for regional water resource management. The results validate the effectiveness of GRACE satellites in monitoring hydrology in complex and anthropogenically affected watersheds while emphasizing the indispensable role of the TGD as a core infrastructure for hydrological regulation under extreme climatic conditions. These findings provide actionable insights for optimizing water resource management in the TGRA, such as dynamic reservoir scheduling and strengthening drought response policies. The seasonal and drought response patterns of TWSA suggest that the operation of the Three Gorges Dam should adopt adaptive strategies. For example, early water storage during drought warning periods (based on GRACE-DSI trends) and coordinated controlled releases during the rainy season to balance flood control and water storage capacity. Integrating GRACE-derived TWSA data into real-time drought monitoring systems can also improve the accuracy of early warning systems.

It is worth noting that, in addition to data uncertainty, the choice of methodology (such as Gaussian filtering, detrending, and interpolation techniques) may also introduce additional uncertainties. Furthermore, the separation of natural and anthropogenic contributions to TWSA changes relies on the accurate representation of natural processes in the GLDAS simulations, a hypothesis that may struggle to fully capture all complex interactions within the watershed. Future research could integrate more meteorological and hydrological datasets to enhance the understanding of drought impacts and improve the assessment of TWSA. Additionally, in areas significantly affected by human activities, conducting quantitative analyses targeting specific types of human activities could provide a more detailed understanding of the driving factors behind changes in water storage, thereby deepening insights into the dynamics of hydrological processes. Addressing uncertainties in data and analytical methods further will help enhance the validity and applicability of the research findings.

Author Contributions: Y.Z. (Yu Zhang) and Y.Z. (Yi Zhang) conceived and designed the research; Y.Z. (Yu Zhang), S.L., X.W. and Y.L. performed the experiments and analyzed the data; Y.Z. (Yu Zhang) and Y.Z. (Yi Zhang) wrote the paper; Y.W. and Y.Z. (Yulong Zhong) revised the paper. All authors have read and agreed to the published version of the manuscript.

Funding: This research was funded in part by the National Natural Science Foundation of China under Grant No. 42274111, 41931074, and 42274113, and in part by the National Precise Gravity Measurement Facility, Huazhong University of Science and Technology under Grant No. PGMF-2024-P006.

Data Availability Statement: The data presented in this study are available on request from the corresponding author.

Acknowledgments: We thank the Center for Space Research (CSR) at the University of Texas at Austin for providing the RL06 GRACE L2 product, which was essential to this study. Additionally, we acknowledge S.L. for their assistance in data analysis. Finally, we appreciate the valuable feedback from anonymous reviewers that helped improve the quality of this paper.

Conflicts of Interest: The authors declare no conflicts of interest.

References

1. Oki, T.; Kanae, S. Global Hydrological Cycles and World Water Resources. *Science* **2006**, *313*, 1068–1072. [CrossRef] [PubMed]
2. Scanlon, B.R.; Fakhreddine, S.; Rateb, A.; de Graaf, I.; Famiglietti, J.; Gleeson, T.; Grafton, R.Q.; Jobbagy, E.; Kebede, S.; Kolusu, S.R.; et al. Global water resources and the role of groundwater in a resilient water future. *Nat. Rev. Earth Environ.* **2023**, *4*, 87–101. [CrossRef]
3. Xu, N.; Lu, H.; Li, W.; Gong, P. Natural lakes dominate global water storage variability. *Sci. Bull.* **2024**, *69*, 1016–1019. [CrossRef] [PubMed]
4. Cooley, S.W.; Ryan, J.C.; Smith, L.C. Human alteration of global surface water storage variability. *Nature* **2021**, *591*, 78–81. [CrossRef]
5. Yao, F.; Livneh, B.; Rajagopalan, B.; Wang, J.; Crétaux, J.-F.; Wada, Y.; Berge-Nguyen, M. Satellites reveal widespread decline in global lake water storage. *Science* **2023**, *380*, 743–749. [CrossRef]
6. Deng, S.; Zhang, M.; Hou, Y.; Wang, H.; Yu, E.; Xu, Y. Terrestrial Water Storage Dynamics: Different Roles of Climate Variability, Vegetation Change, and Human Activities across Climate Zones in China. *Forests* **2022**, *13*, 1541. [CrossRef]
7. Yang, F.; Liang, L.; Wang, C.; Luo, Z. Attitude Determination for GRACE-FO: Reprocessing the Level-1A SC and IMU Data. *Remote Sens.* **2022**, *14*, 126. [CrossRef]
8. Rodell, M.; Reager, J.T. Water cycle science enabled by the GRACE and GRACE-FO satellite missions. *Nat. Water* **2023**, *1*, 47–59. [CrossRef]
9. Wu, Y.; Zhong, Y.; Liu, S.; Xu, G.; Xiao, C.; Wu, X.; Xie, B.; Li, Z.; Shum, C.K. Hydrogeodesy Facilitates the Accurate Assessment of Extreme Drought Events. *J. Earth Sci.* **2025**, *36*, 347–350. [CrossRef]
10. Duan, A.; Zhong, Y.; Xu, G.; Yang, K.; Tian, B.; Wu, Y.; Bai, H.; Hu, E. Quantifying the 2022 extreme drought in the Yangtze River Basin using GRACE-FO. *J. Hydrol.* **2024**, *630*, 130680. [CrossRef]
11. Xu, G.; Liu, S.; Cheng, S.; Zhang, Y.; Wu, X.; Wu, Y. Quantifying the 2022 drought and spatiotemporal evolution of TWSA in the Dongting Lake Basin over the past two decades. *Geod. Geodyn.* **2024**, *15*, 516–527. [CrossRef]
12. Xu, L.; Chen, N.; Zhang, X.; Chen, Z. Spatiotemporal Changes in China's Terrestrial Water Storage From GRACE Satellites and Its Possible Drivers. *J. Geophys. Res. Atmos.* **2019**, *124*, 11976–11993. [CrossRef]
13. Yang, P.; Xia, J.; Zhan, C.; Qiao, Y.; Wang, Y. Monitoring the spatio-temporal changes of terrestrial water storage using GRACE data in the Tarim River basin between 2002 and 2015. *Sci. Total Environ.* **2017**, *595*, 218–228. [CrossRef] [PubMed]
14. Long, D.; Pan, Y.; Zhou, J.; Chen, Y.; Hou, X.; Hong, Y.; Scanlon, B.R.; Longuevergne, L. Global analysis of spatiotemporal variability in merged total water storage changes using multiple GRACE products and global hydrological models. *Remote Sens. Environ.* **2017**, *192*, 198–216. [CrossRef]
15. Zhang, J.; Liu, K.; Wang, M. Seasonal and Interannual Variations in China's Groundwater Based on GRACE Data and Multisource Hydrological Models. *Remote Sens.* **2020**, *12*, 845. [CrossRef]
16. Chen, Y.; Le, Y.; Zhang, D.; Wang, Y.; Qiu, Z.; Wang, L. A photon-counting LiDAR bathymetric method based on adaptive variable ellipse filtering. *Remote Sens. Environ.* **2021**, *256*, 112326. [CrossRef]
17. Li, S.; Ma, J.; Wu, Y.; Xiang, Z.; Bian, S.; Zhai, G. SSS Small Target Detection via Combining Weighted Sparse Model With Shadow Characteristics. *IEEE Trans. Geosci. Remote Sens.* **2023**, *61*, 1–11. [CrossRef]
18. Vignudelli, S.; Birol, F.; Benveniste, J.; Fu, L.-L.; Picot, N.; Raynal, M.; Roinard, H. Satellite Altimetry Measurements of Sea Level in the Coastal Zone. *Surv. Geophys.* **2019**, *40*, 1319–1349. [CrossRef]
19. Martínez-Moreno, J.; Hogg, A.M.; England, M.H.; Constantinou, N.C.; Kiss, A.E.; Morrison, A.K. Global changes in oceanic mesoscale currents over the satellite altimetry record. *Nat. Clim. Change* **2021**, *11*, 397–403. [CrossRef]
20. Xie, J.; Xu, Y.-P.; Wang, Y.; Gu, H.; Wang, F.; Pan, S. Influences of climatic variability and human activities on terrestrial water storage variations across the Yellow River basin in the recent decade. *J. Hydrol.* **2019**, *579*, 124218. [CrossRef]
21. Guo, H.; Hu, Q.; Zhang, Q.; Feng, S. Effects of the Three Gorges Dam on Yangtze River flow and river interaction with Poyang Lake, China: 2003–2008. *J. Hydrol.* **2012**, *416–417*, 19–27. [CrossRef]
22. Liu, S.; Wu, Y.; Xu, G.; Cheng, S.; Zhong, Y.; Zhang, Y. Characterizing the 2022 Extreme Drought Event over the Poyang Lake Basin Using Multiple Satellite Remote Sensing Observations and In Situ Data. *Remote Sens.* **2023**, *15*, 5125. [CrossRef]
23. Xie, Y.-h.; Yue, T.; Xin-sheng, C.; Feng, L.; Zheng-miao, D. The impact of Three Gorges Dam on the downstream eco-hydrological environment and vegetation distribution of East Dongting Lake. *Ecohydrology* **2015**, *8*, 738–746. [CrossRef]

24. Wang, J.; Sheng, Y.; Gleason, C.J.; Wada, Y. Downstream Yangtze River levels impacted by Three Gorges Dam. *Environ. Res. Lett.* **2013**, *8*, 044012. [CrossRef]
25. Sun, Z.; Huang, Q.; Opp, C.; Hennig, T.; Marold, U. Impacts and Implications of Major Changes Caused by the Three Gorges Dam in the Middle Reaches of the Yangtze River, China. *Water Resour. Manag.* **2012**, *26*, 3367–3378. [CrossRef]
26. Guo, W.-x.; Wang, H.-x.; Xu, J.-x.; Xia, Z.-q. Ecological operation for Three Gorges Reservoir. *Water Sci. Eng.* **2011**, *4*, 143–156. [CrossRef]
27. Haddeland, I.; Heinke, J.; Biemans, H.; Eisner, S.; Flörke, M.; Hanasaki, N.; Konzmann, M.; Ludwig, F.; Masaki, Y.; Schewe, J.; et al. Global water resources affected by human interventions and climate change. *Proc. Natl. Acad. Sci. USA* **2014**, *111*, 3251–3256. [CrossRef]
28. Li, Y.; Zhao, G.; Allen, G.H.; Gao, H. Diminishing storage returns of reservoir construction. *Nat. Commun.* **2023**, *14*, 3203. [CrossRef]
29. Wang, S.; Liu, H.; Yu, Y.; Zhao, W.; Yang, Q.; Liu, J. Evaluation of groundwater sustainability in the arid Hexi Corridor of Northwestern China, using GRACE, GLDAS and measured groundwater data products. *Sci. Total Environ.* **2020**, *705*, 135829. [CrossRef]
30. Yang, P.; Xia, J.; Zhan, C.; Wang, T. Reconstruction of terrestrial water storage anomalies in Northwest China during 1948–2002 using GRACE and GLDAS products. *Hydrol. Res.* **2018**, *49*, 1594–1607. [CrossRef]
31. Bibi, S.; Zhu, T.; Rateb, A.; Scanlon, B.R.; Kamran, M.A.; Elnashar, A.; Bennour, A.; Li, C. Benchmarking multimodel terrestrial water storage seasonal cycle against Gravity Recovery and Climate Experiment (GRACE) observations over major global river basins. *Hydrol. Earth Syst. Sci.* **2024**, *28*, 1725–1750. [CrossRef]
32. Dankwa, S.; Zheng, W.; Gao, B.; Li, X. Terrestrial Water Storage (TWS) Patterns Monitoring in the Amazon Basin Using Grace Observed: Its Trends and Characteristics. In Proceedings of the IGARSS 2018—2018 IEEE International Geoscience and Remote Sensing Symposium, Valencia, Spain, 22–27 July 2018; pp. 768–771.
33. Li, F.; Wang, Z.; Chao, N.; Song, Q. Assessing the Influence of the Three Gorges Dam on Hydrological Drought Using GRACE Data. *Water* **2018**, *10*, 669. [CrossRef]
34. Ferreira, V.G.; Yong, B.; Tourian, M.J.; Ndehedehe, C.E.; Shen, Z.; Seitz, K.; Dannouf, R. Characterization of the hydro-geological regime of Yangtze River basin using remotely-sensed and modeled products. *Sci. Total Environ.* **2020**, *718*, 137354. [CrossRef]
35. Chao, N.; Jin, T.; Cai, Z.; Chen, G.; Liu, X.; Wang, Z.; Yeh, P.J.F. Estimation of component contributions to total terrestrial water storage change in the Yangtze river basin. *J. Hydrol.* **2021**, *595*, 125661. [CrossRef]
36. Wang, L.; Kaban, M.K.; Thomas, M.; Chen, C.; Ma, X. The Challenge of Spatial Resolutions for GRACE-Based Estimates Volume Changes of Larger Man-Made Lake: The Case of China's Three Gorges Reservoir in the Yangtze River. *Remote Sens.* **2019**, *11*, 99. [CrossRef]
37. Lai, Y.; Zhang, B.; Yao, Y.; Li, J. Quantitatively Analyzing the Impacts of Seasonal Water Storage Changes in the Three Gorges Reservoir on Nearby Crust. *Pure Appl. Geophys.* **2022**, *179*, 817–831. [CrossRef]
38. Zhang, M.; Teng, Y.; Jiang, Y.; Yin, W.; Wang, X.; Zhang, D.; Liao, J. Evaluation of Terrestrial Water Storage Changes over China Based on GRACE Solutions and Water Balance Method. *Sustainability* **2022**, *14*, 11658. [CrossRef]
39. Yan, X.; Zhang, B.; Yao, Y.; Yin, J.; Wang, H.; Ran, Q. Jointly using the GLDAS 2.2 model and GRACE to study the severe Yangtze flooding of 2020. *J. Hydrol.* **2022**, *610*, 127927. [CrossRef]
40. Ma, W.; Zhou, H.; Dai, M.; Tang, L.; Xu, S.; Luo, Z. Characterizing the drought events in Yangtze River basin via the insight view of its sub-basins water storage variations. *J. Hydrol.* **2024**, *633*, 130995. [CrossRef]
41. Hersbach, H.; Bell, B.; Berrisford, P.; Hirahara, S.; Horányi, A.; Muñoz-Sabater, J.; Nicolas, J.; Peubey, C.; Radu, R.; Schepers, D.; et al. The ERA5 global reanalysis. *Q. J. R. Meteorol. Soc.* **2020**, *146*, 1999–2049. [CrossRef]
42. Li, X.; Zhong, B.; Chen, J.; Li, J.; Wang, H. Investigation of 2020–2022 extreme floods and droughts in Sichuan Province of China based on joint inversion of GNSS and GRACE/GFO data. *J. Hydrol.* **2024**, *632*, 130868. [CrossRef]
43. Yan, X.; Zhang, B.; Yao, Y.; Yang, Y.; Li, J.; Ran, Q. GRACE and land surface models reveal severe drought in eastern China in 2019. *J. Hydrol.* **2021**, *601*, 126640. [CrossRef]
44. Du, M.; Huang, S.; Singh, V.P.; Leng, G.; Huang, Q.; Li, Y. Quantifying the effects of direct human activities and climate change on the spatial propagation of hydrological drought in the Yellow River Basin, China. *J. Hydrol.* **2024**, *643*, 131931. [CrossRef]
45. Huang, Y.; Salama, M.S.; Krol, M.S.; Su, Z.; Hoekstra, A.Y.; Zeng, Y.; Zhou, Y. Estimation of human-induced changes in terrestrial water storage through integration of GRACE satellite detection and hydrological modeling: A case study of the Yangtze River basin. *Water Resour. Res.* **2015**, *51*, 8494–8516. [CrossRef]
46. Wang, L.; Zhu, M.; Zhong, Y.; Sun, J.; Peng, Z. Impacts of artificial dams on terrestrial water storage changes and the Earth's elastic load response during 1950–2016: A case study of medium and large reservoirs in Chinese mainland. *Geod. Geodyn.* **2024**, *15*, 252–263. [CrossRef]

47. Liu, Z.; Chao, N.; Chen, G.; Zhang, G.; Wang, Z.; Li, F.; Ouyang, G. Changes in monthly surface area, water level, and storage of 194 lakes and reservoirs in the Yangtze River Basin during 1990–2021 using multisource remote sensing data. *Sci. Total Environ.* **2024**, *944*, 173840. [CrossRef]
48. Jekeli, C. Alternative methods to smooth the Earth's gravity field. In *Reports of the Department of Geodetic Science and Surveying*; Report No. 327; Ohio State University: Columbus, OH, USA, 1981.
49. Swenson, S.; Wahr, J. Post-processing removal of correlated errors in GRACE data. *Geophys. Res. Lett.* **2006**, *33*, L08402. [CrossRef]
50. Duan, X.J.; Guo, J.Y.; Shum, C.K.; van der Wal, W. On the postprocessing removal of correlated errors in GRACE temporal gravity field solutions. *J. Geod.* **2009**, *83*, 1095–1106. [CrossRef]
51. Qin, P.; Xu, H.; Liu, M.; Du, L.; Xiao, C.; Liu, L.; Tarroja, B. Climate change impacts on Three Gorges Reservoir impoundment and hydropower generation. *J. Hydrol.* **2020**, *580*, 123922. [CrossRef]
52. Tapley, B.D.; Watkins, M.M.; Flechtner, F.; Reigber, C.; Bettadpur, S.; Rodell, M.; Sasgen, I.; Famiglietti, J.S.; Landerer, F.W.; Chambers, D.P.; et al. Contributions of GRACE to understanding climate change. *Nat. Clim. Change* **2019**, *9*, 358–369. [CrossRef]
53. Kornfeld, R.P.; Arnold, B.W.; Gross, M.A.; Dahya, N.T.; Klipstein, W.M.; Gath, P.F.; Bettadpur, S. GRACE-FO: The Gravity Recovery and Climate Experiment Follow-On Mission. *J. Spacecr. Rocket.* **2019**, *56*, 931–951. [CrossRef]
54. Yi, S.; Sneeuw, N. Filling the Data Gaps Within GRACE Missions Using Singular Spectrum Analysis. *J. Geophys. Res. Solid Earth* **2021**, *126*, e2020JB021227. [CrossRef]
55. Chen, J.L.; Wilson, C.R.; Li, J.; Zhang, Z. Reducing leakage error in GRACE-observed long-term ice mass change: A case study in West Antarctica. *J. Geod.* **2015**, *89*, 925–940. [CrossRef]
56. Mo, X.; Wu, J.J.; Wang, Q.; Zhou, H. Variations in water storage in China over recent decades from GRACE observations and GLDAS. *Nat. Hazards Earth Syst. Sci.* **2016**, *16*, 469–482. [CrossRef]
57. Syed, T.H.; Famiglietti, J.S.; Rodell, M.; Chen, J.; Wilson, C.R. Analysis of terrestrial water storage changes from GRACE and GLDAS. *Water Resour. Res.* **2008**, *44*, W02433. [CrossRef]
58. Shouzhang, P. 1 km monthly temperature and precipitation dataset for China from 1901 to 2017. *Earth Syst. Sci. Data* **2019**, *11*, 1931–1946. [CrossRef]
59. Wahr, J.; Molenaar, M.; Bryan, F. Time variability of the Earth's gravity field: Hydrological and oceanic effects and their possible detection using GRACE. *J. Geophys. Res. Solid Earth* **1998**, *103*, 30205–30229. [CrossRef]
60. Wahr, J.; Swenson, S.; Zlotnicki, V.; Velicogna, I. Time-variable gravity from GRACE: First results. *Geophys. Res. Lett.* **2004**, *31*, L11501. [CrossRef]
61. Cui, L.; Zhang, C.; Yao, C.; Luo, Z.; Wang, X.; Li, Q. Analysis of the Influencing Factors of Drought Events Based on GRACE Data under Different Climatic Conditions: A Case Study in Mainland China. *Water* **2021**, *13*, 2575. [CrossRef]
62. Zhang, J.; Liu, K.; Wang, M. Downscaling Groundwater Storage Data in China to a 1-km Resolution Using Machine Learning Methods. *Remote Sens.* **2021**, *13*, 523. [CrossRef]
63. Liu, F.; Kang, P.; Zhu, H.; Han, J.; Huang, Y. Analysis of Spatiotemporal Groundwater-Storage Variations in China from GRACE. *Water* **2021**, *13*, 2378. [CrossRef]
64. Xie, J.; Xu, Y.-P.; Booij, M.J.; Guo, Y. Influences of reservoir operation on terrestrial water storage changes detected by GRACE in the Yellow River basin. *J. Hydrol.* **2022**, *610*, 127924. [CrossRef]
65. Nie, N.; Zhang, W.; Chen, H.; Zhao, D.; Liu, M. Temporal variation characteristics and attribution analysis of terrestrial water storage change in the Yangtze River basin. *Adv. Water Sci.* **2021**, *32*, 396–407. [CrossRef]
66. Cui, L.; Zhu, C.; Wu, Y.; Yao, C.; Wang, X.; An, J.; Wei, P. Natural- and Human-Induced Influences on Terrestrial Water Storage Change in Sichuan, Southwest China from 2003 to 2020. *Remote Sens.* **2022**, *14*, 1369. [CrossRef]
67. Xu, G.; Wu, Y.; Liu, S.; Cheng, S.; Zhang, Y.; Pan, Y.; Wang, L.; Dokuchits, E.Y.; Nkwazema, O.C. How 2022 extreme drought influences the spatiotemporal variations of terrestrial water storage in the Yangtze River Catchment: Insights from GRACE-based drought severity index and in-situ measurements. *J. Hydrol.* **2023**, *626*, 130245. [CrossRef]
68. Zhang, D.; Liu, X.; Li, X.; Bai, P.; Li, J. Assessing changes in total water storage in two large freshwater lake basins of China. *Hydrol. Process.* **2022**, *36*, e14556. [CrossRef]
69. Zhong, Y.; Bai, H.; Feng, W.; Lu, J.; Humphrey, V. Separating the Precipitation- and Non-Precipitation- Driven Water Storage Trends in China. *Water Resour. Res.* **2023**, *59*, e2022WR033261. [CrossRef]
70. Niu, X. The Three Gorges Project. *Engineering* **2022**, *15*, 17–23. [CrossRef]
71. Wang, X.; de Linage, C.; Famiglietti, J.; Zender, C.S. Gravity Recovery and Climate Experiment (GRACE) detection of water storage changes in the Three Gorges Reservoir of China and comparison with in situ measurements. *Water Resour. Res.* **2011**, *47*, W12502. [CrossRef]

Disclaimer/Publisher's Note: The statements, opinions and data contained in all publications are solely those of the individual author(s) and contributor(s) and not of MDPI and/or the editor(s). MDPI and/or the editor(s) disclaim responsibility for any injury to people or property resulting from any ideas, methods, instructions or products referred to in the content.